nature genetics

Nova regulates brain-specific splicing to shape the synapse

Jernej Ule[1], Aljaž Ule[2], Joanna Spencer[1], Alan Williams[3], Jing-Shan Hu[3], Melissa Cline[3], Hui Wang[3], Tyson Clark[3], Claire Fraser[1], Matteo Ruggiu[1], Barry R Zeeberg[4], David Kane[5], John N Weinstein[4], John Blume[3] & Robert B Darnell[1]

Alternative RNA splicing greatly increases proteome diversity and may thereby contribute to tissue-specific functions. We carried out genome-wide quantitative analysis of alternative splicing using a custom Affymetrix microarray to assess the role of the neuronal splicing factor Nova in the brain. We used a stringent algorithm to identify 591 exons that were differentially spliced in the brain relative to immune tissues, and 6.6% of these showed major splicing defects in the neocortex of *Nova2*$^{-/-}$ mice. We tested 49 exons with the largest predicted Nova-dependent splicing changes and validated all 49 by RT-PCR. We analyzed the encoded proteins and found that all those with defined brain functions acted in the synapse (34 of 40, including neurotransmitter receptors, cation channels, adhesion and scaffold proteins) or in axon guidance (8 of 40). Moreover, of the 35 proteins with known interaction partners, 74% (26) interact with each other. Validating a large set of Nova RNA targets has led us to identify a multi-tiered network in which Nova regulates the exon content of RNAs encoding proteins that interact in the synapse.

Human cells contain ~20,000–25,000 genes[1], which would generate a proteome of limited complexity if each gene produced one protein. Alternative RNA splicing is believed to be a primary means of increasing proteome complexity[2] and thereby functional diversity, an issue of particular importance in the brain and immune system. The mechanisms and importance of splicing regulation in mammalian tissues are poorly understood in comparison with the well-explored signaling pathways that regulate transcription of functionally coherent sets of genes[3–6]. Understanding the biologic role of alternative splicing has been impeded by the difficulty in systematically identifying and validating transcripts that are coregulated by specific splicing factors[7]. A few studies have reported splicing defects of small numbers of transcripts in mice lacking RNA-binding proteins[8–11], but no study has undertaken a genome-wide analysis to address statistically the functional coherence of genes coregulated at the level of alternative splicing. Microarrays using exon-junction probes were used first for genome-wide analysis in yeast[12] and then to detect alternative splicing differences in mammalian tissues with a validity rate of ~50% (ref. 13) to 70–85% (refs. 14,15).

The first mammalian tissue-specific splicing factors described were Nova1 and Nova2, neuron-specific KH-type RNA binding proteins[8,16,17]. A limited set of validated Nova splicing targets have been identified through a series of experiments involving Nova-RNA structural studies[18,19], Nova knockout mice[8], RNA cross-linking and immunoprecipitation (CLIP) to determine sites of Nova-RNA contact *in vivo*[9] and biochemical analysis of Nova-regulated splicing[20,21]. Taken together, these studies suggested that Nova might preferentially target RNAs encoding proteins with roles in neuronal inhibition[9]. To address this hypothesis systematically, we undertook a genome-wide screen to identify and validate Nova-dependent alternatively spliced transcripts in brain.

RESULTS

Quantitative analysis of tissue-specific splicing

We analyzed alternative splicing in brains of *Nova2*$^{-/-}$ and *Nova1*$^{-/-}$ mice using a custom Affymetrix microarray previously developed as a prototype to quantify splicing changes of TPM2 and CD44 in human tissues[22]. The microarray contained 40,443 exon junction probe sets derived from 7,175 genes with one or more bioinformatically predicted alternative transcripts. To analyze the data, we developed a simple algorithm (called analysis of splicing by isoform reciprocity, ASPIRE) to identify reciprocal splicing changes between two samples (normalized to steady-state levels; **Fig. 1** and **Supplementary Fig. 1** online). This approach allowed us to identify changes in alternative splicing with high sensitivity and to discriminate them from changes in RNA stability. Data were quantified as the change in the fraction of exon inclusion (ΔI), where a ΔI value of 0.5 indicates a 50% increase and a ΔI value of −0.5 indicates a 50% decrease in exon inclusion in the first of the two compared samples.

[1]Howard Hughes Medical Institute and Laboratory of Molecular Neuro-Oncology, The Rockefeller University, New York, New York, USA. [2]Faculty of Economics and Econometrics, University of Amsterdam, Netherlands. [3]Affymetrix Inc., 6550 Vallejo Street, Suite 100, Emeryville, California, USA. [4]Laboratory of Molecular Pharmacology, National Cancer Institute, National Institutes of Health, Bethesda, Maryland, USA. [5]SRA International Inc., 4300 Fair Lakes Ct., Fairfax, Virginia 22033, USA. Correspondence should be addressed to R.B.D. (darnelr@rockefeller.edu).

Published online 24 July 2005; doi:10.1038/ng1610

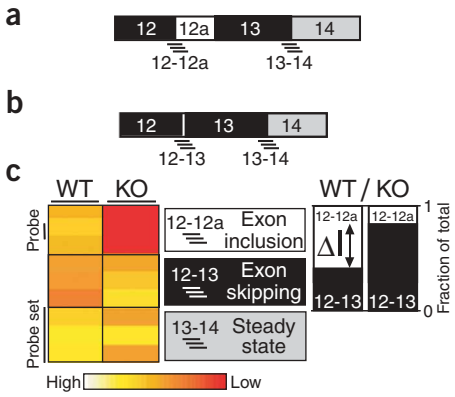

Figure 1 Microarray probe design and ASPIRE method for data analysis. (**a**,**b**) A schematic representation of *Aplp2* alternative isoforms, in which each exon junction and exon body are tiled with probes (as shown in **Supplementary Fig. 1** online). Each alternatively spliced transcript includes probes that recognize the constitutive regions shared between the two reciprocal isoforms (*e.g.*, junction 13-14) and probes that recognize the alternative regions of the exon 12a-including isoform (*e.g.*, junction 12-12a) and the exon 12a-skipping isoform (*e.g.*, junction 12-13). (**c**) A heat map shows the log intensities of three probe sets used for calculation of *Aplp2* exon 12a inclusion in wild-type (WT) and *Nova2*$^{-/-}$ (KO) neocortex. The average signal of all the constitutive probe sets (such as 13-14) was used to calculate the steady-state change and to normalize the signals of the alternative probe sets. The signal of the probe sets recognizing the two reciprocal isoforms changes in opposite direction when exon 12a inclusion decreases in the knockout sample relative to the wild-type sample. The algorithm to calculate the change in fraction of exon inclusion (ΔI) is based on the decrease in probe set 12-12a and increase in probe set 12-13 normalized signals between the two compared samples (wild-type versus knockout).

We did pairwise comparisons of exon usage in brains of Nova knockout mice relative to those of wild-type mice and between different brain and immune tissues (**Fig. 2**) and identified 4,776 differentially spliced exons from 3,008 genes. To define a limit for significant ΔI values, we analyzed tissues that were not expected to show splicing changes; we compared neocortex in wild-type versus Nova1 knockout mice and thymus in wild-type versus Nova2 knockout mice, because neocortex does not express Nova1 (ref. 17) and thymus does not express Nova2. In this analysis we found only one change of $|\Delta I| > 0.20$ that occurred in both comparisons (average $|\Delta I| \approx 0.05$, $R^2 = 0.03$; **Fig. 2a**). Therefore, we used a cutoff of $|\Delta I| > 0.20$ for further analysis. We compared splicing in brain with splicing in immune tissues and identified 1,239 changes with $|\Delta I| > 0.2$ that were common to both spinal cord–thymus and midbrain-thymus comparisons (average $|\Delta I| \approx 0.23$, $R^2 = 0.94$; **Fig. 2b**). When we expanded this analysis to compare splicing in all brain regions with splicing in either thymus or spleen, we found that 12% (591 of 4,776) of exons showed the same differential splicing pattern in all comparisons ($|\Delta I| > 0.2$; **Supplementary Figs. 2** and **3** online). This observation supports predictions of previous studies[13,14] that different brain regions share a pattern of alternative splicing regulation and that this pattern is distinct from that seen in other tissues. These data raise the question of what role neuronal RNA binding proteins have in brain-specific RNA regulation.

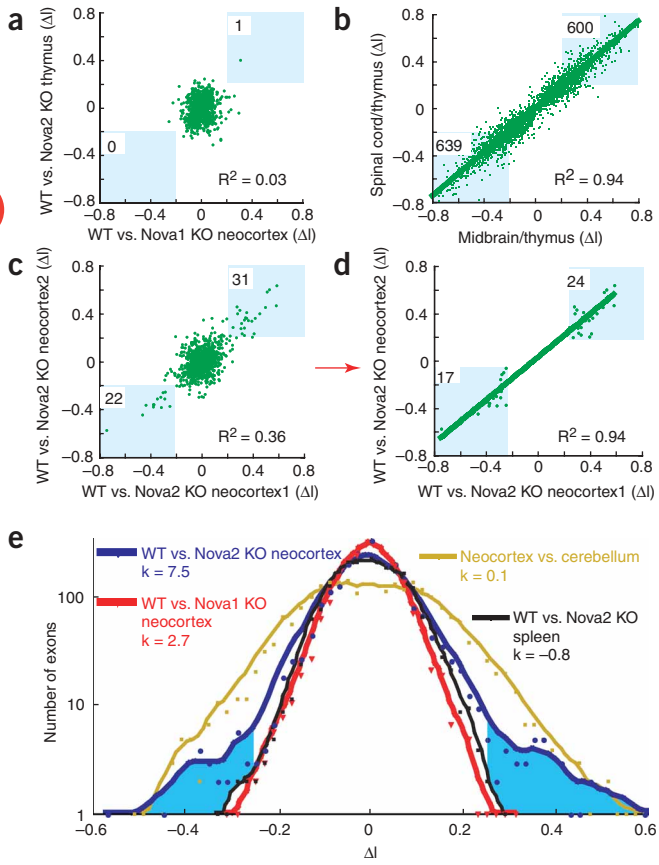

Figure 2 Comparative analysis of microarray data. (**a**–**d**) The splicing changes (ΔI) from one sample comparison are plotted against changes from a second sample comparison to analyze the fraction of data with shared variance (R^2). Blue boxes and numbers indicate the exons with splicing changes in both samples ($|\Delta I| < 0.2$). Comparisons include a negative control (**a**), a positive control (**b**) and comparison of changes detected in two independent sets of triplicate wild-type (WT) versus Nova2 knockout (KO) neocortex samples. A conservative subset of these changes are highlighted in **d** by showing only exons with $|\Delta I| > 0.24$ in the first triplicate sample. (**e**) The distribution of exons as a function of splicing change (ΔI). The distribution of ΔI was divided into intervals of 0.02 width, from ΔI of −0.6 to +0.6 (corresponding to decreased or increased exon inclusion in the first of the two samples, respectively). Each point represents the number of exons in an interval. Kurtosis (k) is a mathematical depiction of the size of a distribution's tails; $k > 3$ represents a distribution with significant outliers; $k \leq 3$ represent normal distributions. Blue shading marks the significant outliers in the distribution of wild-type versus Nova2 knockout neocortex splicing changes.

Nova2 regulates ~7% of brain-specific splicing in the neocortex

Expression of Nova1 and Nova2 is restricted to the central nervous system[16]. In postnatal brain, their expression is largely reciprocal, most obviously in the neocortex where Nova2 is nearly exclusively expressed[17]. We undertook pairwise comparisons between two biologic triplicate samples of neocortex from wild-type and Nova2 knockout mice. We found 53 exons with $|\Delta I| > 0.20$ in both samples (**Fig. 2c**). Moreover, all 41 exons with $\Delta I > 0.24$ in one triplicate correlated ($R^2 = 0.94$) with predicted changes in the second triplicate (**Fig. 2d** and **Supplementary Fig. 3** online). These splicing changes did not follow a normal distribution but affected a specific subset of alternative exons (kurtosis > 3; **Fig. 2e**). In other sample comparisons, the broad spectrum of splicing changes fell on a normal distribution

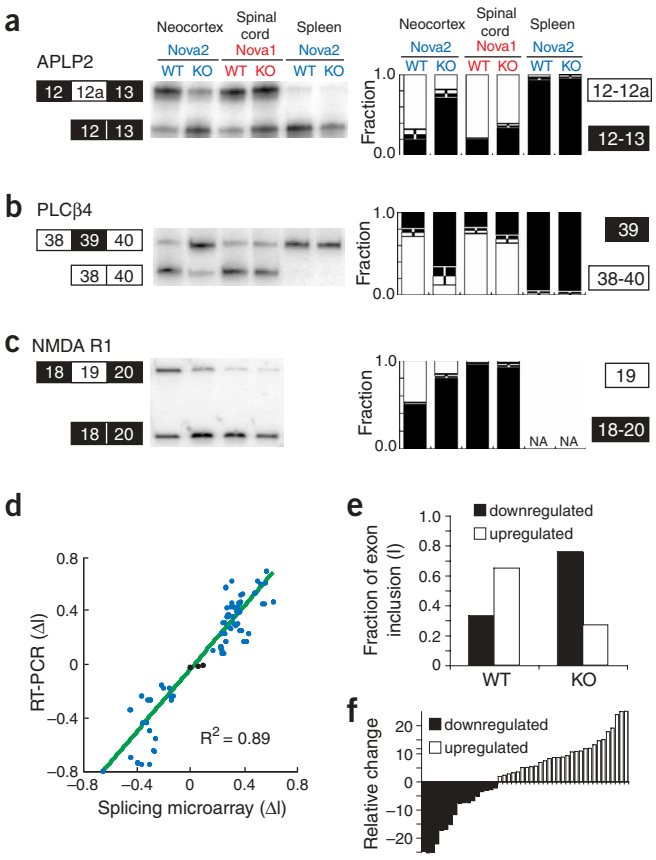

Figure 3 Validation of microarray data by RT-PCR. (**a**–**c**) RT-PCR analysis of three representative Nova-regulated alternative exons. Quantification of triplicate data with error bars (standard deviations) is shown, where black bars represent the spliced isoform downregulated by Nova (which is often the predominant non-neuronal isoform) and white bars represent the spliced isoform upregulated by Nova (often the predominant neuronal isoform). (**c**) NMDAR1 is not expressed in spleen. KO, knockout; WT, wild-type. (**d**) Comparison of ΔI values predicted by microarray and RT-PCR experiment. The positive and negative values represent exons that are up- and downregulated by Nova2, respectively, and the three values close to 0 (black) show exons that are not regulated by Nova2. (**e**) Average fraction of exon inclusion (as determined by RT-PCR) in wild-type (WT) versus Nova2 knockout (KO) neocortex of exons down- (black) and upregulated (white) by Nova. (**f**) The relative change in the alternative isoform ratio in comparison of wild-type versus Nova2 knockout neocortex is shown for all Nova-regulated exons (as determined by RT-PCR).

(kurtosis ≤ 3; **Fig. 2e** and **Supplementary Fig. 3** online), which may be due to noise (*e.g.*, wild-type versus Nova2 knockout spleens) or differences in multiple splicing factors between tissues (*e.g.*, neocortex versus cerebellum). The distribution of splicing changes in neocortex in wild-type versus Nova2 knockout mice (kurtosis = 7.8) indicates that a few transcripts are changed owing to one crucial factor, the absence of Nova2 (**Fig. 2e**), rather than a combination of multiple indirect factors.

We used RT-PCR as an independent assay to examine splicing changes with predicted $|\Delta I| > 0.2$ in both triplicate wild-type versus Nova2 knockout neocortex experiments ($n = 53$; **Fig. 2c**). We identified 36 such exons in well-characterized transcripts (excluding EST and RIKEN sequences) and obtained RT-PCR data for 35 of them (**Fig. 3**, **Table 1** and **Supplementary Fig. 4** online). We also tested 14 exons with less robust changes ($|\Delta I| \geq 0.15$ in at least one experiment; **Table 1**). RT-PCR results for all 49 exons confirmed the direction and magnitude of splicing change predicted by the microarray, with a high statistical correlation between the quantitative predictions of the two methods ($R^2 = 0.89$; **Fig. 3d** and **Table 1**). The ability to predict splicing changes with this accuracy depended on the ASPIRE technique, because traditional statistical methods yielded much lower rates of predicting validated splicing changes (39% by ANOVA and 20% by PAC[22]; data not shown). The average change in the percentage of exon inclusion detected by RT-PCR in wild-type versus Nova2 knockout neocortex was 40% ($\Delta I = 0.4$; **Fig. 3e**). When measured as relative change in the ratio of reciprocal alternative isoforms, 45% of changes were greater than tenfold and 78% were greater than fivefold (**Fig. 3f** and **Table 1**). As a control, we found that 37 of 39 exons predicted to be unchanged ($|\Delta I| < 0.1$) in wild-type versus Nova2 knockout neocortex or Nova1 spinal cord were also unchanged in RT-PCR analysis ($|\Delta I| < 0.1$), and 2 showed small changes ($0.1 < |\Delta I| \leq 0.15$; **Table 1**). In conclusion, all the exons with large predicted change ($|\Delta I| > 0.2$) and 95% of the exons with no predicted change ($|\Delta I| < 0.1$) could be validated by RT-PCR.

Previous studies suggested that Nova has an important role in regulating brain-specific splicing of several transcripts[8,9,20,21]. Of the 49 Nova2-regulated transcripts validated in this study, 31 are expressed both in brain and in immune tissues. Of these, 97% (30/31) have the same splicing pattern in *Nova2*$^{-/-}$ neocortex as in immune tissues, suggesting that Nova2 promotes brain-specific splicing (**Table 1** and **Fig. 3a**,**b**). We also reanalyzed the full set of 591 exons that were differentially spliced in brain relative to immune tissues and found that 6.6% (39 of 591) were Nova-dependent (($|\Delta I|$ wild-type versus Nova2 knockout neocortex) > ($|\Delta I|$ brain versus thymus)/2; **Supplementary Fig. 5** online). Although we did not analyze other nonbrain tissues, our results suggest that Nova helps establish ~7% of differential splicing in the brain.

Strategies for Nova-dependent regulation of splicing

Previous studies found that Nova is able to regulate splicing of cassette or mutually exclusive exons[8,9,20]. Here we identified a number of additional ways in which Nova regulates alternative splicing. Examples among validated Nova2 target RNAs include upregulated use of a terminal exon and an alternative 3′ slice site (*Gpr45* exon 2 and *Idh3b* exon 12, respectively), as well as downregulated use of alternative 3′ and 5′ splice sites (*Ank3* exon 17 and *Ncdn* exon 1, respectively; **Table 1** and **Supplementary Fig. 6** online). We also identified instances where Nova2 regulated two distant (7–40 kb apart) alternatively spliced exons in the same pre-mRNA (*Falz* exons 4 and 9); in some cases, the two exons are regulated in opposite directions (*Chl1* exons 7a and 24; *Epim* exons 8 and 10; **Table 1**). These data indicate that Nova regulates splice-site selection by a variety of mechanisms and, in some cases, may coordinately regulate different functions of a single gene.

We analyzed Nova-dependent splicing regulation in different brain regions. Of the 49 exons with validated splicing change in wild-type versus Nova2 knockout neocortex, 33 also had predicted splicing changes in all other *Nova2*$^{-/-}$ brain regions (**Supplementary Figs. 1** and **3** online). Furthermore, 7 of the 49 validated Nova2 target exons also had predicted splicing change in wild-type versus Nova1 knockout spinal cord, cerebellum and midbrain (validated by RT-PCR; $|\Delta I| > 0.10$; **Table 1**). An example is the Nova-dependent regulation of exon 12a of *Aplp2* (**Fig. 4** and **Supplementary Fig. 1** online). The effects seen in *Nova2*$^{-/-}$ and *Nova1*$^{-/-}$ spinal cord, cerebellum and midbrain are attenuated (relative to wild-type versus Nova2 knockout neocortex), an effect that may be due to redundant action of the two Nova proteins.

Table 1 Validated Nova2-regulated alternative exons

			WT vs. Nova2 KO cx					WT vs. Nova1 KO sc			
			ΔI					ΔI			
Gene symbol	Exon	Function in synapse or axon growth cone	Chip	Chip	PCR		Change	Chip	PCR	cx/sc ΔI	br/nbr ΔI
Agrn	31b	Receptor localization	0.20	0.27	0.24	↑	3.4	0.01	−0.01	−0.02	**0.14**
Agrn	31a	Receptor localization	0.40	0.45	0.24	↑	8		−0.02	−0.06	**0.29**
Ank3	17	Receptor localization	−0.36	−0.44	−0.73	↓	47	0.00	**−0.13**	0.04	**−0.35**
Aplp2	12a	Cell-cell adhesion	0.46	0.49	0.54	↑	12	0.14	**0.16**	−0.05	**0.70**
Arhgap21	8	No data in brain	0.37	0.42	0.18	↑	2.3		0.01	**0.19**	
Atp2b1	35	Neurotransmitter release	0.56	0.56	0.70	↑	34	0.15	**0.20**	0.09	**0.88**
Atp2b1	34	Neurotransmitter release	0.61	0.61	0.47	↑	23		**0.18**	**0.15**	**0.95**
Camk2g	13a	Signaling	0.28	0.30	0.28	↑	3.2				**0.59**
Cask	19	Neurotransmitter release		0.27	0.36	↑	9	0.01			**0.86**
Ctnna2	17a	Receptor localization	−0.25	−0.29	−0.55	↓	12		−0.02	−0.01	
Cacna1b	24a	Neurotransmitter release	0.59	0.51	0.46	↑	9	−0.02	0.04	−0.12	
Chl1	24	Cell-cell adhesion	0.28	0.33	0.36	↑	13	0.03	−0.08	**0.23**	
Chl1	7a	Cell-cell adhesion	−0.57	−0.75	−0.79	↓	127	−0.03	0.02	−0.06	
Clasp1	9	Cytoskeleton binding	0.37	0.34	0.44	↑	7		0.03	**0.20**	**0.62**
Clstn1	10	Signaling	0.34	0.39	0.40	↑	27		0.00	0.01	**0.66**
Dnajb5	1a	Chaperone	0.35	0.33	0.12	↑	51		0.00	**0.12**	
Efna5	3a	Cell-cell adhesion	−0.23	−0.10	−0.17	↓	3.0		0.03	−0.08	
Epha5	4a	Cell-cell adhesion	0.29	0.24	0.58	↑	15	0.02	0.05	**0.13**	**0.38**
Epb4.1	15	Receptor localization		0.22	0.14	↑	1.8	0.31	**0.15**	−0.01	**0.23**
Epb4.1	13	Receptor localization	0.10	0.23	0.11	↑	2.0	0.06	0.04	−0.01	**0.23**
Epb4.1l2	17b	Receptor localization	0.30	0.30	0.44	↑	11	0.06	−0.07	−0.26	**0.41**
Epb4.1l2	17c	Receptor localization	0.34	0.32	0.30	↑	8.6	−0.01	−0.09	−0.37	**0.34**
Epb4.1l3	17c	Receptor localization	0.32	0.31	0.31	↑	11	0.02	0.09	**0.11**	**0.49**
Epim	10	No data in brain	−0.18	−0.11	−0.26	↓	7	−0.01	−0.08	**0.20**	**−0.22**
Falz	4	Transcription	0.22	0.22	0.13	↑	5	0.14	**0.11**	0.04	**0.16**
Golga4	22a	No data in brain	0.25	0.23	0.09	↑	5	0.05	0.03	0.03	**0.15**
Gphn	7a	Receptor localization		−0.45	−0.69	↓	59	−0.04	−0.07	−0.03	**−0.73**
Gpr45	2	No data in brain	−0.30	−0.33	−0.74	↓	50	0.01	0.08	0.00	
Grik2	16	Neurotransmitter receptor	−0.14		−0.23	↓	2.8		0.06	**−0.25**	**−0.74**
Grin1	19	Neurotransmitter receptor		0.25	0.32	↑	5	0.06	0.00	**0.45**	**0.46**
Idh3b	12	No data in brain	0.46	0.27	0.53	↑	15	−0.02	−0.06	0.05	0.00
Igsf4a	8	Cell-cell adhesion	−0.36	−0.38	−0.23	↓	7	−0.03	**−0.15**	−0.05	**−0.48**
Kcnma1	24a	Neurotransmitter release	0.34	0.36	0.40	↑	6		0.00	−0.09	
Kcnq2	13	Neurotransmitter release	0.26		0.18	↑	2.7		−0.02	**0.59**	
Lrp12	7	No data in brain		0.30	0.63	↑	19	−0.01	0.06	**0.24**	**0.55**
Lrp1b	79	No data in brain	0.21	0.39	0.47	↑	11	0.03	0.02	0.06	
Map4k4	22a	Signaling	−0.15	−0.29	−0.15	↓	2.1				**−0.23**
Ncdn	1	No data in brain	−0.31	−0.29	−0.26	↓	17	−0.06	−0.04	**−0.18**	**−0.25**
Ntng1	5a	Axon guidance		0.32	0.26	↑	3.5		0.04	−0.05	
Plcb4	36a	Signaling	−0.25	−0.31	−0.64	↓	22	−0.03	−0.07	0.02	**−0.73**
Ptprf	19a	Receptor localization	0.47	0.58	0.61	↑	18		−0.01	**0.12**	**0.24**
Rap1ga1	27	Signaling	−0.44	−0.47	−0.33	↓	5	−0.03		0.18	
Skip	10	No data in brain	0.41	0.35	0.26	↑	9	0.16	**0.21**	−0.21	**0.19**
Spna2	4	Receptor localization	0.36	0.35	0.46	↑	12	0.06		−0.20	
Srr	2	NMDAR regulation	−0.37	−0.25	−0.49	↓	15	−0.08	0.00	**−0.56**	**−0.41**
Stxbp2	3	Neurotransmitter release	−0.14	−0.17	−0.23	↓	2.8	−0.00	0.06	**−0.25**	**−0.74**
Tacc2	10	No data in brain	0.36	0.19	0.38	↑	5	0.13	0.07	**0.41**	**0.63**
Tpm3	6b	Cytoskeleton binding	0.24	0.31	0.43	↑	7			−0.18	**0.53**
Tpm3	6a	Cytoskeleton binding	−0.31	−0.35	−0.43	↓	7				**−0.60**

Comparison of splicing predictions made by two independent triplicate microarray experiments (chip) and RT-PCR (PCR) results for the 49 alternative exons that were assayed by both methods. Splicing change is shown as ΔI for wild-type (WT) versus Nova2 knockout (KO) neocortex (cx), wild-type versus Nova1 knockout spinal cord (sc) and neocortex versus spinal cord and for comparison of all brain regions versus spleen and thymus (br/nbr). Values for exons that change in the same direction as in wild-type versus Nova2 knockout neocortex are shown in bold. The relative change in the alternative isoform ratio in wild-type versus Nova2 knockout neocortex is also shown. For genes with described synaptic functions, the primary function is listed (supporting references are available from our project website). The exons are numbered on the basis of the representative mRNAs in the mm3 mouse genome.

Finally, we identified five transcripts with Nova-dependent differential splicing in the cortex and spinal cord. These encode NMDA NR1 subunit (**Fig. 3c**), KCNQ2 potassium channel, serine racemase, Hsc40 and Arhgap21 (**Table 1**). These observations suggest that, in addition to regulating brain-specific splicing, in some cases Nova also contributes to differential splicing between brain regions.

Nova regulates splicing of RNAs encoding synaptic functions

To examine the types of function encoded by Nova-regulated transcripts, we used the program GoMiner[23], which allowed us to apply statistical measures to this analysis. We used an improved version of GoMiner that replicates genes by the number of regulated alternative exons in the gene and carries out multiple sample comparisons to determine the false discovery rate (FDR)[24]. These studies suggested that Nova preferentially regulates transcripts encoding proteins that function in the synapse. We compared the gene functions associated with Nova-regulated exons ($n = 48$; **Table 1**) with those associated with the complete set of microarray alternative exons from genes expressed in brain ($n = 2{,}710$). Functions with the most significant enrichment among Nova-regulated transcripts ($P < 0.001$, FDR < 0.03, 6- to 13-fold enrichment; **Table 2**) were synapse biogenesis and synaptic transmission, cell-cell signaling, cortical actin organization (*i.e.*, arrangement of actin just beneath the plasma membrane), cell adhesion and extracellular matrix organization. Notably, all these proteins act at the cell membrane, most often at the cell-cell junctions, suggesting they may all act in the synapse. Other enriched functions ($P < 0.02$, FDR < 0.2, three- to sixfold enrichment; **Table 2**) were also synapse-related, including ion transport, regulation of synaptic plasticity, regulation of cell shape, axonogenesis and neurite morphogenesis. We also examined the relative representation of exons in 14 biological functions (representing 72% (35 of 48) of the validated Nova targets and 61% (242 of 397) of the exons differentially spliced between brain and immune tissues). We found that 88% of the Nova-regulated exons, compared with only 24% of the control exons, encode synapse-related functions ($P < 0.01$; **Fig. 4**). By contrast, only 8% of Nova-regulated genes, compared with 68% of control exons, encode proteins that are not identified as acting directly in the synapse according to Gene Ontology annotation (**Fig. 4**).

Table 2 Gene Ontology functions of alternatively spliced exons

		WT vs. Nova2 KO neocortex			Brain/immune tissues			Spleen/thymus		
	Total exons	Exons	*P*	FDR	Exons	*P*	FDR	Exons	*P*	FDR
Biological process	2,710	48			412			133		
Synapse organization and biogenesis	40	8	<0.001	<0.001	10	0.015	0.169	3		
Extracellular matrix organization	50	9	<0.001	<0.001	14	0.003	0.051	3		
Neurogenesis	256	17	<0.001	<0.001	62	<0.001	<0.001	10		
Cortical actin cytoskeleton organization	19	5	<0.001	<0.001	9	0.001	0.036	2		
Synaptogenesis	36	6	<0.001	0.002	9	0.016	0.18	3		
Cell-cell signaling	170	11	<0.001	0.005	41	<0.001	0.002	5		
Synaptic transmission	108	8	<0.001	0.017	30	<0.001	<0.001	0		
Cell adhesion	206	11	<0.001	0.02	35			6		
Regulation of cell shape	31	4	0.002	0.056	7			2		
Neurite morphogenesis	54	5	0.002	0.057	8			0		
Behavior	67	5	0.006	0.109	11			1		
Ion transport	195	9	0.006	0.122	23			6		
Axonogenesis	45	4	0.008	0.126	8			0		
Regulation of synaptic plasticity	28	3	0.013	0.153	7			3		
Actin filament-based process	102	5	0.033		34	<0.001	<0.001	6		
Organelle organization and biogenesis	351	7			78	<0.001	0.002	20		
Cell motility	99	4			25	0.001	0.042	1		
Cytokinesis	33	0			13	0.001	0.044	1		
Rho protein signal transduction	21	0			9	0.003	0.065	1		
Microtubule-based process	74	1			18	0.004	0.073	3		
Cell differentiation	134	2			32	0.004	0.08	14	0.004	0.114
Cell cycle	233	1			49	0.008	0.102	10		
Vesicle-mediated transport	142	1			32	0.008	0.104	4		
Lymphocyte differentiation	31	0			6			9	<0.001	<0.001
Immune response	170	0			33			23	<0.001	<0.001
Chromatin modification	43	0			3			9	<0.001	0.008
B-cell differentiation	20	0			3			6	<0.001	0.009
Steroid metabolism	38	0			3			6	0.006	0.104
Regulation of Pol II transcription	100	0			14			12	0.005	0.11

Representation of functions defined by Gene Ontology Biological Process categories and analyzed by GoMiner. Six hundred and fifty Gene Ontology categories had 15–400 total exons, and we show all those (barring redundant ontologies) for which statistically significant results were obtained (FDR < 0.16, $P < 0.02$). The significance of enrichment in experimental relative to control set is indicated by *P* value (one-sided Fisher exact test) and FDR (*P* value corrected for multiple comparisons). The total number of exons from genes expressed in brain (total), the 48 Nova regulated exons (wild-type (WT) versus Nova2 knockout (KO) neocortex) validated here and in previous studies[8,9], and the exons with predicted differential splicing in brain versus immune tissues ($|\Delta I| > 0.2$ in all possible comparisons) or in spleen versus thymus ($|\Delta I| > 0.24$) are shown. Comparison of regulation by alternative splicing and by steady state is shown in **Supplementary Table 2** online.

Because the Gene Ontology annotation is incomplete, we searched PubMed and identified clearly defined brain-related functions for 40 of the 49 proteins encoded by Nova target transcripts validated in this study. Although multiple functions are ascribed to many of these proteins, 85% (34 of 40) function in synaptic transmission and plasticity, and 20% (8 of 40) function in axonogenesis (**Table 1**). Of the 40 proteins, 7 are involved in neurotransmitter release, 2 are neurotransmitter receptors, 7 are cell-cell adhesion proteins, 11 regulate localization of receptors and other membrane proteins, and 6 are signal transducers (**Table 1**). Moreover, 35 of the 40 proteins have known protein-protein interactions, and 74% of these 35 proteins (26 of 35) interact with each other (**Fig. 5**). These data identify a multitiered network in which Nova-regulated RNAs encode proteins that interact in the synapse.

General functions of tissue-specific alternative splicing

We undertook a more general analysis of functions among genes with tissue-specific splicing patterns in comparison with the total set of tissue-expressed genes. Functions with most significant enrichment ($P < 0.001$, FDR < 0.03, two- to threefold enrichment; **Table 2** and **Fig. 4**) among genes differentially spliced between brain and immune tissues were synaptic transmission, cell-cell signaling, neurogenesis, actin-filament and microtubule-based process, and organelle organization. Those with most significant enrichment among genes differentially spliced between spleen and thymus were lymphocyte and B-cell differentiation, immune response and chromatin modification.

We found no significant (more than twofold) steady-state changes in wild-type versus Nova2 knockout neocortex (**Supplementary Figs. 1** and **2** online), including those transcripts whose alternative splicing is regulated by Nova2. More generally, whereas many genes showed large differences in steady-state levels in brain relative to thymus and spleen (**Supplementary Fig. 2** online), there was no correlation between changes in steady-state level and splicing changes in any of the sample comparisons ($R^2 < 0.01$; data not shown). These data agree with previous studies showing that alternative splicing acts independently of transcription to define tissue-specific expression profiles[14,15] and show that Nova does not have a general role in regulating gene transcription or RNA turnover.

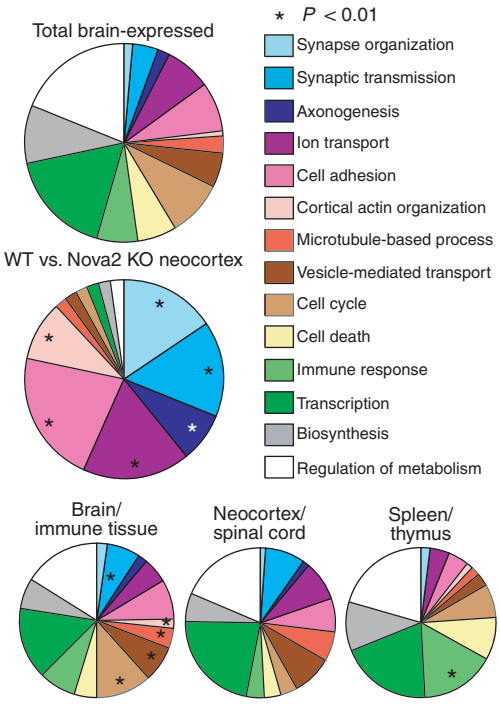

Figure 4 Relative representation of selected Gene Ontology functions for the total set of control exons from genes expressed in brain that were tested on the microarray (total brain-expressed); the 54 Nova2 regulated exons (wild-type (WT) versus Nova2 knockout (KO) neocortex) validated to date (including five previously reported[8,9]); and the exons predicted to be differentially spliced in brain versus immune tissues (shared $|\Delta I| > 0.2$), in neocortex versus spinal cord ($|\Delta I| > 0.24$) and in spleen versus thymus ($|\Delta I| > 0.24$). The numerical data underlying this figure are shown in **Table 2**. The genes with potential synaptic functions (blue, purple) represent 24% of control exons and 88% of Nova-target genes ($P < 0.01$). Eight percent of Nova-regulated genes, compared with 68% of control exons, encode proteins that are not known to act locally at the synapse.

DISCUSSION

Here we report the first genome-wide analysis to our knowledge of alternative splicing in a mouse model of a human disorder, POMA. We used mice lacking Nova, a neuron-specific RNA-binding protein identified as the POMA antigen, to identify and validate a large array of Nova-regulated alternative exons. This analysis identified Nova as a regulatory protein at the top of a hierarchical network. Nova coregulates alternative splicing of RNAs encoding synaptic proteins that interact among themselves (**Fig. 5**). POMA is believed to relate to defective neuronal inhibition; therefore, it is of particular interest that Nova targets relate to inhibitory synaptic function.

We identified nine Nova-regulated exons for transcripts encoding neurotransmitter receptors or proteins that regulate neurotransmitter release, in addition to two such proteins that were previously identified[8] (**Table 1** and **Fig. 5**). Nova also regulates transcripts encoding adhesion, scaffold and signaling proteins, indicating that Nova may contribute to regulation of functional and structural synaptic changes that underlie synaptic plasticity. Nova regulates transcripts encoding proteins that may be implicated in a previously undiscovered long-term potentiation (LTP) of slow inhibitory postsynaptic current (sIPSC) that follows the activation of NMDA receptors[25]. These include RNAs encoding NMDAR1, necessary for LTP of both excitatory postsynaptic current and sIPSC[25]; GIRK2 potassium channel and GABAB2 receptor[9], which give rise to sIPSC[25]; CaMKIIγ, which transmits signals to potassium channels[26]; CASK and neurochondrin, which inhibit CaMKII[27,28]; and PLCβ4, which degrades PIP2, a mediator of receptor-dependent activation of GIRK[29]. Nova2 function is necessary for the induction of LTP of sIPSC in hippocampal neurons[25]. These data suggest that in intact brain, modulation of Nova activity may modify the ability of synapses to induce or maintain inhibitory plasticity, where Nova contributes to the higher-order regulation called 'metaplasticity'[30].

We identified 12 Nova-regulated exons for transcripts encoding proteins that regulate localization of receptors and other membrane proteins (**Table 1** and **Fig. 5**)[9]. Notably, Nova regulates splicing of all members of the spectrin–ankyrin–protein 4.1–CASK scaffold complex that functions as a linker between membrane proteins and the actin-tropomyosin cytoskeleton, and this complex is implicated in the subcellular organization of the GABAergic synapse[31]. CLIP experiments previously showed that Nova binds β-spectrin and protein 4.1N RNAs[9], and we now find that Nova regulates splicing of RNAs encoding α-spectrin and three additional members of the protein 4.1 family (**Table 1**). These observations suggest that Nova-regulated splicing of 4.1R and its homologs contributed to the functional diversification of this protein family[32]. Furthermore, Nova promotes inclusion of an exon in protein 4.1R that encodes part of the

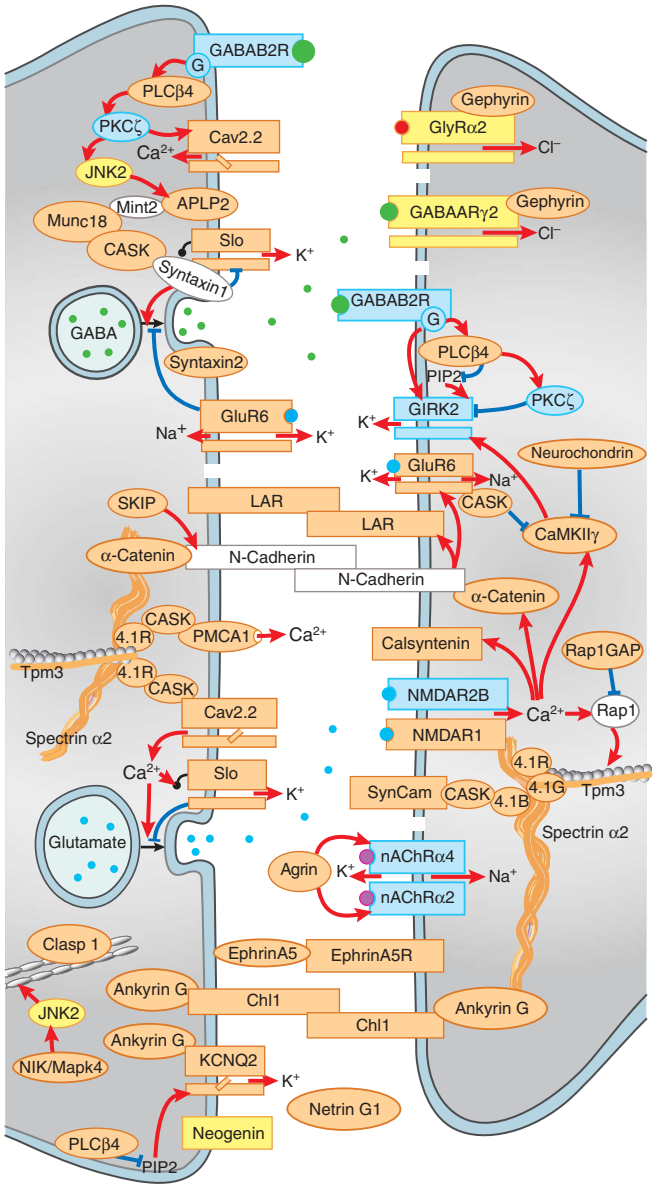

Figure 5 The synaptic module of 41 proteins encoded by validated Nova-regulated RNAs (see also **Table 1**). The proteins encoded by validated RNAs identified by the microarray are shown in orange, and those validated in previous studies[8,9] are shown in yellow. Proteins encoded by RNAs identified by multiple Nova CLIP tags[9] are shown in blue, and other proteins in the same networks that are not known to be regulated by Nova are shown in white. Red arrows denote positive regulatory interactions, and blue bars denote negative regulatory interactions. All proteins shown are not necessarily present in a single synapse (symbolized by interruptions in the membranes). The references for each interaction are available from our project website.

spectrin-fodrin-actin interacting domain[33], and transcripts encoding α-spectrin are in turn subject to Nova-dependent splicing regulation.

Another illustration of Nova-regulated targets that are functionally linked to each other is those associated with the neuromuscular junction. Nova upregulates inclusion of exons 32 and 33 in agrin mRNA (Z+ isoforms), which are made in neurons and are necessary for agrin to cluster nicotinic acetylcholine receptors (nAChR) at the neuromuscular junction and stimulate synapse formation[34]. Moreover, RNAs encoding both nAChR subunits α4 and β2 were previously identified multiple times by CLIP tags in exon 5 of both genes[9], suggesting that Nova may coordinately regulate nAChR function in the neuromuscular junction or the central nervous system.

We identified seven Nova-regulated exons for transcripts encoding adhesion proteins (**Table 1** and **Fig. 5**). One of these, SynCAM, can stimulate synapse formation when used to transfect non-neuronal cells[35]. Two other proteins, EphA5 and ephrin-A5, have a key role in excluding limbic thalamic afferents from the sensorimotor cortex by mediating repulsive interactions[36]. Previous studies of EphA7, another ephrin-A5 receptor, found that two alternative isoforms of EphA7 receptors stimulate cell adhesion versus repulsion[37]. By analogy, Nova regulation of alternative splicing may affect the outcome of ephrin-A5–EphA5 interaction, which may in turn affect axon guidance and hippocampal LTP[36].

Probe sets for only one previously reported Nova splicing target, *Gphn* exon 9, were present on the microarray, and our results here were concordant with our previous analysis[9] (**Table 1**). Ninety-nine genes that were tested on the microarray contained Nova CLIP tags, and none other than *Gphn* showed $|\Delta I|$ values >0.20. But 95 of these were CLIP tags in 3′ untranslated regions or long introns (far from known alternative exons); these Nova CLIP tags may relate to functions other than splicing regulation. Moreover, the methods are fundamentally different, as CLIP yields RNAs directly bound by Nova, whereas the microarray identifies Nova-dependent splicing targets regardless of whether they are directly bound by Nova. Additional biochemical and biostatistical analysis will be required to address this issue. Nonetheless, the two very different techniques yielded functionally convergent data, as 71% of the RNAs with multiple CLIP tags encoded synaptic functions.

Genome-wide analysis of gene expression has focused on transcriptional control, and some transcription factors are believed to regulate clusters of genes encoding similar functions (modules), including genes involved in neuronal function[3–6]. Cellular networks may depend on such encapsulation of functions within modules in order to increase the robustness and flexibility of cells[38]. One of the first indications that such coordinate regulation may also occur at the RNA level were findings in fruit flies that sex lethal regulates splicing or translation of several transcripts involved in sex determination (tra, sxl and msl-2)[39,40] and findings in mammalian cells that the iron-regulatory RNA binding proteins mediate translational regulation of IRE-containing mRNAs (ferritin, transferring, ferropoetin and others)[41]. More recently, suggestions of additional regulatory RNA networks have arisen from studies in which *in vitro* selection or coprecipitation experiments were used to identify RNA-protein interactions in yeast[42,43], fruit flies[44], mammalian tissue-culture cells[45,46] and the brain[9,47,48].

The Nova-regulated network identified here provides the first description to our knowledge of a validated regulatory module operating at the level of information content mediated by RNA exon usage. This network seems to be especially robust, given the large number of validated exons, the coherent functions of the encoded proteins and the interactions among these proteins. Our data shows that the steady-state levels of Nova-regulated RNAs are unchanged in knockout versus wild-type brains, underscoring the nature of regulated alternative exon usage as a means of modulating the quality of synaptic protein interactions. Rather than the quantitative nature afforded by control of steady-state transcript or protein expression, the modular control of exon usage stands out as a qualitative means of regulating information content.

This new kind of network required new analytic approaches. We used kurtosis to measure the distribution of predicted splicing changes, leading to the conclusion that Nova regulates a small subset of alternatively spliced exons, consistent with a modular regulatory structure. We also used GoMiner to analyze the functions of Nova targets by considering exons, rather than whole genes, as individual units (**Table 2**). Our ASPIRE method differed in several ways from standard microarray analysis. We filtered the data of individual probes using statistical measures of variance before generating probe sets and empirically optimized filtering criteria that gave high prediction validity. We then identified probe set pairs for reciprocal alternative isoforms bioinformatically and searched for reciprocal signal changes between biological samples (**Fig. 1**). We found that quantifying the splicing as change in fraction of alternative exon inclusion (ΔI) gives a higher prediction validity (a near 100% validity rate for $\Delta I > 0.20$) than relative change in alternative isoform ratios, although we provide both types of quantification for comparison (**Fig. 3e,f**). Taken together, this tailoring of our analysis to alternative exon usage allowed us to develop a robust means of identifying Nova targets.

In summary, we identified a new gene regulatory module consisting of transcripts coregulated at the level of alternative splicing. Nova-regulated transcripts encode proteins that form an interaction module in the synapse (**Fig. 5**). Such splicing regulatory modules may have provided a means for coordinate regulation of neuron-specific functions to evolve in the context of a genome of limited size.

METHODS

Microarray design. A custom Affymetrix mouse microarray[49] was designed to comprehensively monitor all alternative splicing events predicted on the basis of alignment of mouse cDNA sequences from dbEST (2 April 2002), RefSeq (2 April 2002) and GenBank (2 April 2002) to the draft assembly of the mouse genome (30 November 2001; Whitehead). We consolidated the cDNA alignments into a nonredundant set of splice variants using altMerge[50]. We identified alternatively spliced exons and then tiled a series of probe sets to interrogate those splicing events. The design of the microarray enabled analysis of cassette exons or alternate splice donors or acceptors. For alternative transcripts, we designed perfect match probe sets for sequence regions unique to each transcript to generate unique probe sets. For constitutive regions that monitor steady-state expression of the gene, we designed perfect match probe sets for sequence regions occurring in a maximal number of transcripts from the same gene.

Most probe sets consisted of six 25-mer perfect match probes spanning the exon-exon junction (40,443 exon junction probe sets in total). We tiled the 25-mer probes with the center probe position (base 13) at positions −3, −2, −1, 1, 2 and 3 relative to the exon-exon junction. We derived the junction probe sequence from the mouse genomic sequence, 15 bases flanking each side of the intron. The microarray also contained exon body probe sets, derived from the mouse genomic sequence contained in the exon, consisting of ten 25-mer perfect match probes selected using the Affymetrix probe hybridization model.

Target preparation, hybridization, array washing and scanning. We reverse-transcribed 5 μg of total RNA from postnatal day 7 mouse brain or immune tissues using random hexamers. We purified cDNA, fragmented it to a length of ~50–200 nucleotides using deoxyribonuclease I and end-labeled it with a biotin-conjugated nucleotide using terminal transferase. We hybridized the labeled target to the arrays for 16 h at 50 °C in 7% dimethylsulfoxide. We washed and stained the probe arrays in an Affymetrix Fluidics Station using standard protocols for eukaryotic targets. We scanned the stained and washed chips on a GeneArray Scanner (Agilent Technologies). Details are given in **Supplementary Methods** online.

ASPIRE. We used different cDNA amounts for each replicate microarray experiment (ranging from 1.9 μg to 4.2 μg), and so we normalized the background-subtracted signal intensity of individual probes to the total signal intensity, such that the average spot intensity was the same for all experiments. We filtered the resulting data with a number of quality control criteria that required low variability between replicates and mean and median values above defined cutoff values (**Supplementary Methods** online) so that only high-quality probe data were retained. We filtered the data relative to two samples that were compared, rather than the whole set of data, in a way that retained probes that had high signal intensity in one sample, even if the other sample had low intensity. In this way, probes that potentially represent alternative splicing changes were retained. We then normalized the probe intensities of each gene relative to the change in steady-state level of the gene, using the signals of probes recognizing constitutive parts of the transcript. We generated probe set values by calculating the median signal intensity of probes that recognized the same exon-exon junction or the same exon body.

We carried out a search algorithm to identify all potential probe set pairs recognizing reciprocal alternative isoforms. On the basis of bioinformatic predictions, we matched each probe set testing an exon junction that skips an alternative exon (**Fig. 1a**) to a probe set testing either the alternative exon body or one of the exon junctions contacting the alternative exon (**Fig. 1b**). To refine the alternative exon predictions, we used pairwise comparative analysis of the raw data from all our samples (Nova knockout and wild-type neocortex, cerebellum, midbrain, spinal cord, thymus and spleen) to find probe set pairs that detected a change in at least one sample. We identified 4,776 probe set pairs, belonging to 3,008 genes, in which the two probe sets recognizing exon-including and exon-skipping isoforms showed greater than 1.4-fold reciprocal change of the normalized signals between any two samples. Therefore, these 4,776 exons were defined by both bioinformatic prediction and preliminary comparative analysis of the data. We quantified the change in fraction of exon inclusion (ΔI) of these 4,776 exons by comparing two samples at a time. We used two algorithms; the one that provided greater stringency was $\Delta I = (1 - \text{Rin})^*(1 - \text{Rex})/(\text{Rex} - \text{Rin})$, where Rin is the ratio of exon-including probe set signal and Rex is the ratio of exon-excluding probe set signal between the two compared samples. Details are given in **Supplementary Methods** online.

Experimental validation of splicing changes. We determined ratios of exon-including isoforms to exon-excluding isoforms by RT-PCR as described previously[8] and, where indicated, by quantitative real-time PCR. Details are given in **Supplementary Methods** online, and primer sequences are given in **Supplementary Table 1** online.

Functional analysis by GoMiner. The genes we analyzed differed in the number of tested alternative exons (from one to nine exons per gene). GoMiner[23] and High-Throughput GoMiner[24] traditionally dereplicate total and changed gene input files so that only one instance of a gene name is processed. When multiple alternatively spliced forms are to be analyzed, however, dereplication would result in a loss of information relevant to alternative splicing. Consequently, we used a new version of High-Throughput GoMiner to retain full information about the alternative splice variants by replicating the input of each gene into GoMiner by the number of alternative exons per gene in total and changed gene input files. We calculated the significance of enrichment in experimental relative to control set (control set being the total set of exons from genes that are expressed in both of the compared samples) as one-sided Fisher exact *P* values and as FDRs. We obtained FDR values using High-Throughput GoMiner by resampling the control set of exons on the microarray 1,000 times (the total brain-expressed set in case of Nova) and comparing the distribution of *P* values in all the categories for the real data and the resampled data. We computed the corrected *P* values as (randoms mean)/(number of categories), which is an approximation of the fraction of categories that, by random chance, would have had a *P* value that was as low as that observed for the real data. Details of High-Throughput GoMiner and the implementation of exon-replicated gene input are available[24].

URL. Our project website is http://splicing.rockefeller.edu/.

Note: Supplementary information is available on the Nature Genetics website.

ACKNOWLEDGMENTS

We thank L.Y. Jan, B. Taneri and Y. Xia for comments on the manuscript; X. Wang for designing the website with the microarray data; S.A. Fung-Ho for help with figure design; A. Titov and T. Vojtko for help with the Pathway Assist

program; and all members of the lab for their help and insight throughout this work. This work was supported by grants from the US National Institutes of Health (R.B.D.) and the Howard Hughes Medical Institute, the tumor immunology program of Cancer Research Institute (J.U.), an MSTP grant (J.S.) and a Human Frontiers Science Program Fellowship (M.R.). R.B.D. is an Investigator of the Howard Hughes Medical Institute.

COMPETING INTERESTS STATEMENT

The authors declare that they have no competing financial interests.

Received 11 April; accepted 17 June 2005
Published online at http://www.nature.com/naturegenetics/

1. International Human Genome Sequencing Consortium. Finishing the euchromatic sequence of the human genome. *Nature* **431**, 931–945 (2004).
2. Black, D.L. Protein diversity from alternative splicing: a challenge for bioinformatics and post-genome biology. *Cell* **103**, 367–370 (2000).
3. Harbison, C.T. *et al.* Transcriptional regulatory code of a eukaryotic genome. *Nature* **431**, 99–104 (2004).
4. McClung, C.A. & Nestler, E.J. Regulation of gene expression and cocaine reward by CREB and DeltaFosB. *Nat. Neurosci.* **6**, 1208–1215 (2003).
5. Livesey, F.J., Furukawa, T., Steffen, M.A., Church, G.M. & Cepko, C.L. Microarray analysis of the transcriptional network controlled by the photoreceptor homeobox gene. Crx. *Curr. Biol.* **10**, 301–310 (2000).
6. Brivanlou, A.H. & Darnell, J.E. Jr. Signal transduction and the control of gene expression. *Science* **295**, 813–818 (2002).
7. Shin, C. & Manley, J.L. Cell signalling and the control of pre-mRNA splicing. *Nat. Rev. Mol. Cell Biol.* **5**, 727–738 (2004).
8. Jensen, K.B. *et al.* Nova-1 regulates neuron-specific alternative splicing and is essential for neuronal viability. *Neuron* **25**, 359–371 (2000).
9. Ule, J. *et al.* CLIP identifies Nova-regulated RNA networks in the brain. *Science* **302**, 1212–1215 (2003).
10. Kanadia, R.N. *et al.* A muscleblind knockout model for myotonic dystrophy. *Science* **302**, 1978–1980 (2003).
11. Xu, X. *et al.* ASF/SF2-regulated CaMKIIdelta alternative splicing temporally reprograms excitation-contraction coupling in cardiac muscle. *Cell* **120**, 59–72 (2005).
12. Clark, T.A., Sugnet, C.W. & Ares, M. Jr. Genomewide analysis of mRNA processing in yeast using splicing-specific microarrays. *Science* **296**, 907–910 (2002).
13. Johnson, J.M. *et al.* Genome-wide survey of human alternative pre-mRNA splicing with exon junction microarrays. *Science* **302**, 2141–2144 (2003).
14. Pan, Q. *et al.* Revealing global regulatory features of mammalian alternative splicing using a quantitative microarray platform. *Mol. Cell* **16**, 929–941 (2004).
15. Le, K. *et al.* Detecting tissue-specific regulation of alternative splicing as a qualitative change in microarray data. *Nucleic Acids Res.* **32**, e180 (2004).
16. Buckanovich, R.J., Yang, Y.Y. & Darnell, R.B. The onconeural antigen Nova-1 is a neuron-specific RNA-binding protein, the activity of which is inhibited by paraneoplastic antibodies. *J. Neurosci.* **16**, 1114–1122 (1996).
17. Yang, Y.Y., Yin, G.L. & Darnell, R.B. The neuronal RNA-binding protein Nova-2 is implicated as the autoantigen targeted in POMA patients with dementia. *Proc. Natl. Acad. Sci. USA* **95**, 13254–13259 (1998).
18. Buckanovich, R.J. & Darnell, R.B. The neuronal RNA binding protein Nova-1 recognizes specific RNA targets *in vitro* and *in vivo*. *Mol. Cell. Biol.* **17**, 3194–3201 (1997).
19. Lewis, H.A. *et al.* Sequence-specific RNA binding by a Nova KH domain: implications for paraneoplastic disease and the fragile X syndrome. *Cell* **100**, 323–332 (2000).
20. Dredge, B.K. & Darnell, R.B. Nova regulates GABA(A) receptor gamma2 alternative splicing via a distal downstream UCAU-rich intronic splicing enhancer. *Mol. Cell. Biol.* **23**, 4687–4700 (2003).
21. Dredge, B.K., Stefani, G., Engelhard, C.C. & Darnell, R.B. Nova autoregulation reveals dual functions in neuronal splicing. *EMBO J.* **24**, 1608–1620 (2005).
22. Wang, H. *et al.* Gene structure-based splice variant deconvolution using a microarray platform. *Bioinformatics* **19** Suppl 1, i315–i322 (2003).
23. Zeeberg, B.R. *et al.* GoMiner: a resource for biological interpretation of genomic and proteomic data. *Genome Biol.* **4**, R28 (2003).
24. Zeeberg, B.R. *et al.* High-Throughput GoMiner, an 'industrial-strength' integrative Gene Ontology tool for interpretation of multiple-microarray experiments, with application to studies of Common Variable Immune Deficiency (CVID). *BMC Bioinformatics* **6**, 168 (2005).
25. Huang, C.S. *et al.* Long-term potentiation of slow synaptic inhibition induced by coincidence detection of excitation in the CA1 pyramidal neuron requires Nova-2 function. *Cell* (in the press).
26. Balla, Z., Hoch, B., Karczewski, P. & Blasig, I.E. Calcium/calmodulin-dependent protein kinase IIdelta 2 and gamma isoforms regulate potassium currents of rat brain capillary endothelial cells under hypoxic conditions. *J. Biol. Chem.* **277**, 21306–21314 (2002).
27. Lu, C.S., Hodge, J.J., Mehren, J., Sun, X.X. & Griffith, L.C. Regulation of the Ca2+/CaM-responsive pool of CaMKII by scaffold-dependent autophosphorylation. *Neuron* **40**, 1185–1197 (2003).
28. Dateki, M. *et al.* Neurochondrin negatively regulates CaMKII phosphorylation and nervous system specific gene disruption results in epileptic seizure. *J. Biol. Chem.* **280**, 20503–20508 (2005).
29. Kobrinsky, E., Mirshahi, T., Zhang, H., Jin, T. & Logothetis, D.E. Receptor-mediated hydrolysis of plasma membrane messenger PIP2 leads to K+-current desensitization. *Nat. Cell Biol.* **2**, 507–514 (2000).
30. Abraham, W.C. & Bear, M.F. Metaplasticity: the plasticity of synaptic plasticity. *Trends Neurosci.* **19**, 126–130 (1996).
31. Ango, F. *et al.* Ankyrin-based subcellular gradient of neurofascin, an immunoglobulin family protein, directs GABAergic innervation at purkinje axon initial segment. *Cell* **119**, 257–272 (2004).
32. Parra, M. *et al.* Differential domain evolution and complex RNA processing in a family of paralogous EPB41 (protein 4.1) genes facilitate expression of diverse tissue-specific isoforms. *Genomics* **84**, 637–646 (2004).
33. Schischmanoff, P.O. *et al.* Defining of the minimal domain of protein 4.1 involved in spectrin-actin binding. *J. Biol. Chem.* **270**, 21243–21250 (1995).
34. Burgess, R.W., Nguyen, Q.T., Son, Y.J., Lichtman, J.W. & Sanes, J.R. Alternatively spliced isoforms of nerve- and muscle-derived agrin: their roles at the neuromuscular junction. *Neuron* **23**, 33–44 (1999).
35. Biederer, T. *et al.* SynCAM, a synaptic adhesion molecule that drives synapse assembly. *Science* **297**, 1525–1531 (2002).
36. Gao, W.Q. *et al.* Regulation of hippocampal synaptic plasticity by the tyrosine kinase receptor, REK7/EphA5, and its ligand, AL-1/Ephrin-A5. *Mol. Cell. Neurosci.* **11**, 247–259 (1998).
37. Holmberg, J., Clarke, D.L. & Frisen, J. Regulation of repulsion versus adhesion by different splice forms of an Eph receptor. *Nature* **408**, 203–206 (2000).
38. Hartwell, L.H., Hopfield, J.J., Leibler, S. & Murray, A.W. From molecular to modular cell biology. *Nature* **402**, C47–C52 (1999).
39. Nagoshi, R.N., McKeown, M., Burtis, K.C., Belote, J.M. & Baker, B.S. The control of alternative splicing at genes regulating sexual differentiation in *D. melanogaster*. *Cell* **53**, 229–236 (1988).
40. Hedley, M.L. & Maniatis, T. Sex-specific splicing and polyadenylation of dsx pre-mRNA requires a sequence that binds specifically to tra-2 protein *in vitro*. *Cell* **65**, 579–586 (1991).
41. Hentze, M.W. & Kuhn, L.C. Molecular control of vertebrate iron metabolism: mRNA-based regulatory circuits operated by iron, nitric oxide, and oxidative stress. *Proc. Natl. Acad. Sci. USA* **93**, 8175–8182 (1996).
42. Hieronymus, H. & Silver, P.A. Genome-wide analysis of RNA-protein interactions illustrates specificity of the mRNA export machinery. *Nat. Genet.* **33**, 155–161 (2003).
43. Gerber, A.P., Herschlag, D. & Brown, P.O. Extensive association of functionally and cytotopically related mRNAs with Puf family RNA-binding proteins in yeast. *PLoS Biol.* **2**, E79 (2004).
44. Kim, S., Shi, H., Lee, D.K. & Lis, J.T. Specific SR protein-dependent splicing substrates identified through genomic SELEX. *Nucleic Acids Res.* **31**, 1955–1961 (2003).
45. Tenenbaum, S.A., Carson, C.C., Lager, P.J. & Keene, J.D. Identifying mRNA subsets in messenger ribonucleoprotein complexes by using cDNA arrays. *Proc. Natl. Acad. Sci. USA* **97**, 14085–14090 (2000).
46. Waggoner, S.A. & Liebhaber, S.A. Identification of mRNAs associated with alphaCP2-containing RNP complexes. *Mol. Cell. Biol.* **23**, 7055–7067 (2003).
47. Darnell, J.C. *et al.* Fragile X mental retardation protein targets G quartet mRNAs important for neuronal function. *Cell* **107**, 489–499 (2001).
48. Brown, V. *et al.* Microarray identification of FMRP-associated brain mRNAs and altered mRNA translational profiles in fragile X syndrome. *Cell* **107**, 477–487 (2001).
49. Fodor, S.P. *et al.* Light-directed, spatially addressable parallel chemical synthesis. *Science* **251**, 767–773 (1991).
50. Wheeler, R. A method of consolidating and combining EST and mRNA alignments to a genome to enumerate supported splice variants. *Lecture Notes in Computer Science* **2452**, 201–209 (2002).